Journal of
Mechanical
Science and
Technology

Journal of Mechanical Science and Technology 21 (2007) 723~736

Investigation of Beam-plate Systems Including Indirect Coupling in Terms of Statistical Energy Analysis

J. W. Yoo [a,*], D. J. Thompson[b], N. S. Ferguson[b]

[a]*Vehicle CAE Team, Vehicle Technology Center, Hyundai-Kia Motors, Jangduk-Dong Hwaseong-Si, 445-706, Korea*
[b]*Institute of Sound and Vibration Research, University of Southampton, Southampton, SO17 1BJ, UK*

(Manuscript Received September 15, 2006; Revised March 26, 2007; Accepted March 27, 2007)

Abstract

Statistical Energy Analysis (SEA) is generally used for the high frequency analysis in various areas. In the present paper a SEA-related study concerning coupled structures consisting of beams and plates is discussed. Firstly, the Fourier technique is explained to obtain the energies and power flows for excitation on the beam and the plate. Then, these are used in the Power Injection Method (PIM) to obtain the effective Coupling Loss Factors (CLFs) of the single beam-plate system. Overlapping octave bands are used in a frequency average approach. Based on the analysis for the beam-plate structure, the beam-plate-beam structure is also investigated in the SEA framework. It is found that the indirect coupling in an SEA sense may exist for such a beam-plate-beam coupled structure. The numerical result shows that its effect is larger when the dimensions of beams are similar.

Keywords: SEA; Coupling loss factor; Fourier technique; Beam; Plate; Indirect coupling; Power injection method

1. Introduction

At high frequencies the dynamic response is increasingly sensitive to structural details (Kompella and Bernhard, 1993) and this means that the exact modelling of a particular system using such as Finite Element Method (FEM) is limited and impractical (Lyon and DeJong, 1995). Thus high frequency analysis should be carried out in a different way, i.e. a statistical approach which provides more useful spatial and frequency average behaviour. The most widely accepted is Statistical Energy Analysis (SEA) (Fahy, 1994), in which the system is considered to be an assembly of subsystems and each subsystem is assigned a single energy degree of freedom (ESDU 99009). The coupling loss factor (CLF) describes the power transferred through a junction between subsystems. SEA is generally used in various areas such as buildings (Craik, 1996), aerospace applications (Jayachandran and Bonilha, 2003) and more recently automotive vehicles (Noguchi et al., 2006).

The present paper deals with beam-plate coupled structures in terms of the SEA framework. Some of previous studies concerning coupled structures consisting of beams and/or plates are here reviewed.

Two line-coupled finite rectangular plates were investigated by Wester and Mace (1996). The response of the system was described using a wave approach. The subsystem was assumed to be drawn from an ensemble. It was shown that the traditional SEA hypothesis of power proportionality is exact for the ensemble average response of the plate systems, regardless of the strength of coupling.

Strasberg and Feit (1996) derived a simple expression for the vibration damping induced by a multitude of small sprung masses without using a probabilistic approach and applied this to a simple

*Corresponding author. Tel.: 82 31 368 3351; Fax.: +82
Fax : 82 31 368 2733
E-mail address: j.w.yoo@hyundai-motor.com

structure consisting of a beam and a plate. From this study it is observed that a so-called fuzzy structure behaves mainly as damping to the master structure and the level of the damping is independent of the dissipation factor of the attachments.

Grice and Pinnington (1999) used a wave analysis to study a built-up structure consisting of a stiff beam and flexible plate in which the beam is seen as a source and the plate as a receiver. If the flexural wavenumber in the plate is at least twice as large as the coupled wavenumber in the beam, the dynamic behaviour of the beam can be described in terms of the locally reacting impedance of the plate

The power mode approach was used to a built-up structure consisting of a stiff beam (source) and a flexible plate (receiver) connected through a discrete coupling (Ji et al., 2003). If the receiver structure is much more flexible than the source, the approximate power transmission can be given simply, incor-porating the mobilities of the uncoupled source and receiver.

As seen, it seems difficult to find SEA-based studies that deal with beam-plate coupled systems. Such evaluation provides the motivation of the present study.

A Fourier approach is introduced in this paper to make numerical models of such beam-plate (-beam) systems. These models satisfy energy conservation (thus power balance). The validity of the numerical model is experimentally shown. In SEA, a complex system is notionally divided into a number of subsystems that are connected through junctions. SEA parameters such as CLFs will depend on how the subsystems are chosen. For a beam-plate coupled structure, the subsystems can conveniently be chosen as the beam and the plate. As the cases in which the external force is applied to the beam and then to the plate are analysed using the Fourier approach, SEA parameters are evaluated for these cases based on the power balance equations.

Although the SEA systems should be evaluated strictly in terms of ensemble averages (Lyon and DeJong, 1995), the application based on the ensemble is often impractical. It is known that the variance of the response over the ensemble decreases when the frequency averaging bandwidth increases (ESDU 99009). Thus, the frequency average technique is used here instead of using the ensemble average. Also predictions of the spatial sum of the energy of a subsystem are made instead of the response at any particular point in the subsystem.

Finally, the effective CLFs obtained for the single beam coupled structure are used in a SEA model to predict the subsystem energies of a beam-plate-beam coupled structure. The SEA model used assumes only direct coupling, i.e. no indirect coupling between the beams. Then, the predicted energies are compared with those calculated exactly with the Fourier technique and discrepancies are noted.

The beams are modelled based on Euler-Bernoulli beam theory and an isotropic plate is assumed. An external point force is applied normal (i.e. z direction) upon the beam or plate. Only flexural motion (in the z direction) for both the beam and plate is taken into account, which is the most important energy-carrying wave. Meanwhile, it may also be expected that transversal or rotational beam motion occurs (i.e. motion in the y direction), which includes rigid behaviours. The transversal motion coupled to the plate in-plane motion would be found relatively at high frequencies where only a few numbers of corresponding modes exist. Especially, under such a loading condition, the energy portion due to the beam rotation would be very small comparing with the flexural motion energy. Thus, one can expect that the present study based on the consideration of only the flexural motion remains reasonable. Note that SEA deals with modal energies, so that a few particular modes are not of concern and no modal energy occurs due to rigid motion. Also note that numerical models in the present study based on only the flexural waves satisfy energy conservation.

2. Analytical model of a beam-plate-beam structure

First of all, in this chapter a numerical model to be used for SEA is introduced. Among various applicable approaches, the present study uses a Fourier method, which can be considered exact for the present boundary condition. A particular coupled system of two beams coupled through a plate is taken into account here and the plate is excited. Note that either a beam-plate system or a beam-excited condition can also be considered instead.

2.1 Motion of the coupled structure

The coupled structure consisting of two infinite beams and an infinitely long finite width plate can be analysed using a Fourier transform technique. The

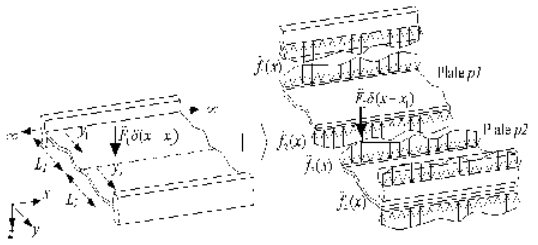

Fig. 1. A built-up structure consisting of infinite two beams attached to an infinitely long finite width plate and the force relationship between them.

corresponding subsystems of such a structure and their force relationships are shown in Fig. 1. Harmonic motion at frequency ω is assumed and the beams are assumed to be infinitely stiff to torsion along $y_1 = 0$ and $y_2 = L_2$.

The external point force is only acting on the plate located at $y_1 = L_1$ and the force is defined by $\tilde{F}_0\delta(x-x_1)\delta(y-L_1)$ where δ is the Dirac delta function. When the infinitely long finite width plate and the infinite beam (beam $b1$) are joined along the line $y_1 = 0$, a force per unit length $f_1(x)$ acts between them as shown in Fig. 1. Now considering all forces related to beam $b1$, the flexural motion of this beam with damping becomes

$$\tilde{D}_b \frac{\partial^4 \tilde{w}_{b1}(x)}{\partial x^4} - m'_{b1}\omega^2 \tilde{w}_{b1}(x) = -\tilde{f}_1(x) \tag{1}$$

where subscript $b1$ stands for beam $b1$, $\tilde{D}_b$ is its complex bending stiffness and m'_{b1} is its mass per unit length. In the same manner, the equation of motion for the other beam (beam $b2$) is

$$\tilde{D}_b \frac{\partial^4 \tilde{w}_{b2}(x)}{\partial x^4} - m'_{b2}\omega^2 \tilde{w}_{b2}(x) = \tilde{f}_4(x). \tag{2}$$

The spatial Fourier transforms of Eqs. (1) and (2) give respectively

$$\tilde{D}_b k_x^4 \tilde{W}_{b1}(k_x) - m'_{b1}\omega^2 \tilde{W}_{b1}(k_x) = -\tilde{F}_1(k_x) \tag{3}$$

$$\tilde{D}_b k_x^4 \tilde{W}_{b2}(k_x) - m'_{b2}\omega^2 \tilde{W}_{b2}(k_x) = \tilde{F}_4(k_x) \tag{4}$$

where $\tilde{W}_{b1}(k_x)$ and $\tilde{W}_{b2}(k_x)$ are the Fourier transformed displacement of beams $b1$ and $b2$ respectively and $\tilde{F}_1(k_x)$ and $\tilde{F}_4(k_x)$ are the Fourier transforms of $\tilde{f}_1(x)$ and $\tilde{f}_4(x)$ respectively.

Also, the equation of flexural motion of the free plate with damping is

$$\tilde{D}_p \left(\frac{\partial^4 \tilde{w}_p(x,y)}{\partial x^4} + 2\frac{\partial^4 \tilde{w}_p(x,y)}{\partial x^2 \partial y^2} + \frac{\partial^4 \tilde{w}_p(x,y)}{\partial y^4} \right) - m''_p \omega^2 \tilde{w}_p(x,y) = 0 \tag{5}$$

where $\tilde{D}_p$ is its complex bending stiffness and m''_p is its mass per unit area of the plate. The corresponding Fourier transform of Eq.(5) is

$$\tilde{D}_p \left\{ k_x^4 \tilde{W}_p(k_x,y) - 2k_x^2 \frac{\partial^2 \tilde{W}_p(k_x,y)}{\partial y^2} + \frac{\partial^4 \tilde{W}_p(k_x,y)}{\partial y^4} \right\} - m'_p \omega^2 \tilde{W}_p(k_x,y) = 0 \tag{6}$$

where $\tilde{W}_p(k_x,y)$ is the Fourier transformed displacement of the plate. If harmonic waves in the plates are assumed, the wavenumber relationship can be defined. For waves of the form $e^{k_y y}e^{ik_x x}$ the wave propagating or decaying away from the junction of beam $b1$ and the plate is defined as

$$k_y = -\sqrt{k_x^2 - \tilde{k}_p^2} = \tilde{k}_{y1}, \tag{7a}$$

$$k_y = -\sqrt{k_x^2 + \tilde{k}_p^2} = \tilde{k}_{y2} \tag{7b}$$

where $\tilde{k}_p$ is the plate free wavenumber. Meanwhile, the positive square roots are assumed for waves travelling towards the junction and are found to be

$$k_y = \sqrt{k_x^2 - \tilde{k}_p^2} = \tilde{k}_{y3}, \tag{7c}$$

$$k_y = \sqrt{k_x^2 + \tilde{k}_p^2} = \tilde{k}_{y4}. \tag{7d}$$

If $|k_x| < |\tilde{k}_p|$, then wavenumbers $\tilde{k}_{y1}$ and $\tilde{k}_{y3}$ are considered as travelling waves, and $\tilde{k}_{y2}$ and $\tilde{k}_{y4}$ are considered as nearfield waves. Conversely, if $|k_x| > |\tilde{k}_p|$, then all of them behave as nearfield waves.

Then the motion of plate $p1$ can be written as

$$\tilde{W}_{p1}(k_x,y_1) = \tilde{B}_1 e^{\tilde{k}_{y1}y_1} + \tilde{B}_2 e^{\tilde{k}_{y2}y_1} + \tilde{B}_3 e^{\tilde{k}_{y3}y_1} + \tilde{B}_4 e^{\tilde{k}_{y4}y_1} \tag{8}$$

and for plate $p2$,

$$\tilde{W}_{p2}(k_x, y_2) = \tilde{C}_1 e^{\tilde{k}_{y1} y_2} + \tilde{C}_2 e^{\tilde{k}_{y2} y_2} + \tilde{C}_3 e^{\tilde{k}_{y3} y_2} + \tilde{C}_4 e^{\tilde{k}_{y4} y_2} \quad (9)$$

Note that different local coordinate systems are used in Eqs. (8) and (9) in describing the motion of the plate i.e. $y_1 (\equiv y)$ for plate $p1$ and $y_2 (\equiv y - L_1)$ for plate $p2$.

The response of the beams and the plates can be obtained based on application of the appropriate boundary conditions.

(i) Continuity equation for beam $b1$ and plate $p1$; equal displacement to the plate at $y_1 = 0$ of plate $p1$

$$\tilde{W}_{p1}(k_x, y_1)\Big|_{y_1=0} = \tilde{W}_{b1}(k_x) \quad (10)$$

(ii) Sliding condition; beam $b1$ is assumed infinitely stiff to torsion along $y_1 = 0$ of plate $p1$

$$\frac{\partial \tilde{W}_{p1}(k_x, y_1)}{\partial y_1}\bigg|_{y_1=0} = 0 \quad (11)$$

(iii) Force equilibrium condition; the force on plate $p1$ are equal and opposite to the respective force on beam $b1$

$$\tilde{D}_p \left[\frac{\partial^3 \tilde{W}_{p1}(k_x, y_1)}{\partial y_1^3} - k_x^2 (2-\nu) \frac{\partial \tilde{W}_{p1}(k_x, y_1)}{\partial y_1} \right]_{y_1=0} = \tilde{F}_1(k_x) \quad (12)$$

(iv) Continuity equation for plate $p1$ and plate $p2$; equal displacement at junction $y_1 = L_1$ of plate $p1$ and $y_2 = 0$ of plate $p2$

$$\tilde{W}_{p1}(k_x, y_1)\Big|_{y_1=L_1} = \tilde{W}_{p2}(k_x, y_2)\Big|_{y_2=0} \quad (13)$$

(v) Continuity equation for plate $p1$ and plate $p2$; equal rotational displacement at junction $y_1 = L_1$ of plate $p1$ and $y_2 = 0$ of plate $p2$

$$\frac{\partial \tilde{W}_{p1}(k_x, y_1)}{\partial y_1}\bigg|_{y_1=L_1} = \frac{\partial \tilde{W}_{p2}(k_x, y_2)}{\partial y_2}\bigg|_{y_2=0} \quad (14)$$

(vi) Moment equilibrium condition; the moments acting on plates $p1$ and $p2$ are equal at junction $y_1 = L_1$

$$\tilde{M}_{p1}(k_x, y_1)\Big|_{y_1=L_1} = \tilde{M}_{p2}(k_x, y_2)\Big|_{y_2=0} \quad (15)$$

where $\tilde{M}_p(k_x, y_i)$ is the Fourier transform of the moment per unit length $\tilde{M}_p(x, y_i)$ acting on edges of a plate and given by

$$\tilde{M}_p(k_x, y_i) = \tilde{D}_p \left[\frac{\partial^2 \tilde{W}_p(k_x, y_i)}{\partial y_i^2} - k_x^2 \nu \tilde{W}_p(k_x, y_i) \right], \quad i = 1, 2. \quad (16)$$

(vii) Force equilibrium condition; the forces acting at junction $y_1 = L_1$ of plate $p1$ and $y_2 = 0$ of plate $p2$ should be in equilibrium with the applied external force as shown in Fig. 1.

$$-\tilde{F}_2(k_x, y_1)\Big|_{y_1=L_1} + \tilde{F}_3(k_x, y_2)\Big|_{y_2=0} = \tilde{F}_0(k_x) \quad (17)$$

where $\tilde{F}_2(k_x, y_1)$, $\tilde{F}_3(k_x, y_2)$ and $\tilde{F}_0(k_x)$ are the Fourier transforms of the forces $\tilde{f}_2(x, y_1)$, $\tilde{f}_3(x, y_2)$ and $\tilde{F}_0(x - x_1)$ respectively.

(viii) Continuity equation for plate $p2$ and beam $b2$; equal displacement to the plate at $y_2 = L_2$ of plate $p2$

$$\tilde{W}_{p2}(k_x, y_2)\Big|_{y_2=L_2} = \tilde{W}_{b2}(k_x) \quad (18)$$

(ix) Sliding condition; beam $b2$ is assumed infinitely stiff to torsion along $y_2 = L_2$ of plate $p2$

$$\frac{\partial \tilde{W}_{p2}(k_x, y_2)}{\partial y_2}\bigg|_{y_2=L_2} = 0 \quad (19)$$

(x) Force equilibrium condition; the force on plate $p2$ are equal and opposite to the respective force on beam $b2$

$$\tilde{D}_p \left[\frac{\partial^3 \tilde{W}_{p2}(k_x, y_2)}{\partial y_2^3} \right.$$

$$-k_x^2(2-\nu)\frac{\partial \tilde{W}_{p2}(k_x,y_2)}{\partial y_2}\Bigg]_{y_2=L_2} = \tilde{F}_4(k_x) \tag{20}$$

The equations representing boundary conditions (10), (11), (12), (13), (14), (15), (17), (18), (19) and (20) can be expressed in a matrix form. The matrix form of the equations in the wavenumber domain is

$$\mathbf{Ku} = \mathbf{F} \tag{21}$$

where the dynamic stiffness matrix $\mathbf{K}$ is

$$\mathbf{K}=\begin{bmatrix}
1 & 1 & 1 & 1 & 0 & 0 & 0 & 0 & -1 & 0 \\
\tilde{k}_{y1} & \tilde{k}_{y2} & \tilde{k}_{y3} & \tilde{k}_{y4} & 0 & 0 & 0 & 0 & 0 & 0 \\
\alpha_1 & \alpha_2 & \alpha_3 & \alpha_4 & 0 & 0 & 0 & 0 & \frac{\tilde{K}_{b1}}{\tilde{D}_p} & 0 \\
e^{\tilde{k}_{y1}L_1} & e^{\tilde{k}_{y2}L_1} & e^{\tilde{k}_{y3}L_1} & e^{\tilde{k}_{y4}L_1} & -1 & -1 & -1 & -1 & 0 & 0 \\
\tilde{k}_{y1}e^{\tilde{k}_{y1}L_1} & \tilde{k}_{y2}e^{\tilde{k}_{y2}L_1} & \tilde{k}_{y3}e^{\tilde{k}_{y3}L_1} & \tilde{k}_{y4}e^{\tilde{k}_{y4}L_1} & -\tilde{k}_{y1} & -\tilde{k}_{y2} & -\tilde{k}_{y3} & -\tilde{k}_{y4} & 0 & 0 \\
\beta_1 e^{\tilde{k}_{y1}L_1} & \beta_2 e^{\tilde{k}_{y2}L_1} & \beta_3 e^{\tilde{k}_{y3}L_1} & \beta_4 e^{\tilde{k}_{y4}L_1} & -\beta_1 & -\beta_2 & -\beta_3 & -\beta_4 & 0 & 0 \\
-\alpha_1 e^{\tilde{k}_{y1}L_1} & -\alpha_2 e^{\tilde{k}_{y2}L_1} & -\alpha_3 e^{\tilde{k}_{y3}L_1} & -\alpha_4 e^{\tilde{k}_{y4}L_1} & \alpha_1 & \alpha_2 & \alpha_3 & \alpha_4 & 0 & 0 \\
0 & 0 & 0 & 0 & e^{\tilde{k}_{y1}L_2} & e^{\tilde{k}_{y2}L_2} & e^{\tilde{k}_{y3}L_2} & e^{\tilde{k}_{y4}L_2} & 0 & -1 \\
0 & 0 & 0 & 0 & \tilde{k}_{y1}e^{\tilde{k}_{y1}L_2} & \tilde{k}_{y2}e^{\tilde{k}_{y2}L_2} & \tilde{k}_{y3}e^{\tilde{k}_{y3}L_2} & \tilde{k}_{y4}e^{\tilde{k}_{y4}L_2} & 0 & 0 \\
0 & 0 & 0 & 0 & \alpha_1 e^{\tilde{k}_{y1}L_2} & \alpha_2 e^{\tilde{k}_{y2}L_2} & \alpha_3 e^{\tilde{k}_{y3}L_2} & \alpha_4 e^{\tilde{k}_{y4}L_2} & 0 & \frac{\tilde{K}_{b2}}{\tilde{D}_p}
\end{bmatrix} \tag{22}$$

where $\tilde{K}_{b1} = \tilde{D}_b k_x^4 - m'_{b1}\omega^2$, $\tilde{K}_{b2} = \tilde{D}_b k_x^4 - m'_{b2}\omega^2$, $\alpha_i = \tilde{k}_{yi}^3 - k_x^2(2-\nu)\tilde{k}_{yi}$ and $\beta_i = \tilde{k}_{yi}^2 - k_x^2\nu$ for $i = 1$, 2, 3, and 4. Also, the displacement vector $\mathbf{u}$ in terms of the wave amplitudes in the plate and the transformed beam displacements is

$$\mathbf{u} = \Big[\tilde{B}_1(k_x)\ \tilde{B}_2(k_x)\ \tilde{B}_3(k_x)\ \tilde{B}_4(k_x)\ \tilde{C}_1(k_x)\ \tilde{C}_2(k_x)\ \tilde{C}_3(k_x)\ \tilde{C}_4(k_x)\ \tilde{W}_{b1}(k_x)\ \tilde{W}_{b2}(k_x)\Big]^T, \tag{23}$$

and the force vector is

$$\mathbf{F} = \Big[0\ 0\ 0\ 0\ 0\ 0\ \tilde{F}_0(k_x)/\tilde{D}_p\ 0\ 0\ 0\Big]^T. \tag{24}$$

Thus, if the excitation force is known, the response of the beams and the plates can be found from the solution of Eq. (21) as follows.

$$\mathbf{u} = \mathbf{K}^{-1}\mathbf{F}\ . \tag{25}$$

As the response of the coupled structure consisting of infinite beams and the infinitely long finite width plate is identified, the response of a finite structure such as the structure shown in Fig. 2 can be obtained based on a Fourier series expansion.

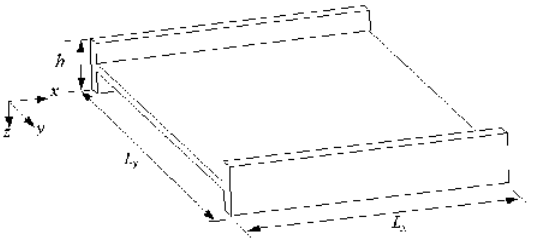

Fig. 2. A built-up structure consisting of two finite beams attached to a rectangular plate.

The response of beam $b1$ that has 'sliding beam ends' is written as

$$\tilde{w}_{b1}(x) = \frac{\tilde{W}_{b1,0}}{2} + \sum_{n=1}^{\infty}\tilde{W}_{b1,n}\cos(k_{x,n}x) \tag{26}$$

where $k_{x,n} = n\pi/L_x$ and $\tilde{W}_{b1,n} = \tilde{W}_{b1}(k_{x,n})$ is the n^{th} component of the motion of the coupled beam $b1$, which is defined in Eq. (25). Similarly, the responses of the other beam and plates could be found using Eq. (26) where $\tilde{W}_{b2}$, $\tilde{W}_{p1}$ and $\tilde{W}_{p2}$ should be used respectively.

The same procedure can be used if an external unit force is applied at a beam. Although the details are not shown here, as there are only six unknowns, the dynamic behaviours of the same waveguide structure consisting of infinite systems can be found. Then the response of the finite coupled system can be obtained using a Fourier series such as Eq. (26) for the sliding beam ends. The dynamic response of a single beam coupled system can be found in a similar manner.

2.2 Experimental verification

The numerical results obtained based on the Fourier transform technique is compared with experiments. Note the in the Fourier technique, the ends of the two beams experience sliding conditions. Meanwhile, in the experiment the boundaries are free, as sliding boundary conditions cannot be realised.

It is clear that extending the range for the Fourier transform in Eq. (26) produces better results. However, it also requires more computational time and thus in the present case, a total of 120 Fourier components is used. These components can describe all possible behaviours in the frequency of interest

(5.6 – 1412 Hz)

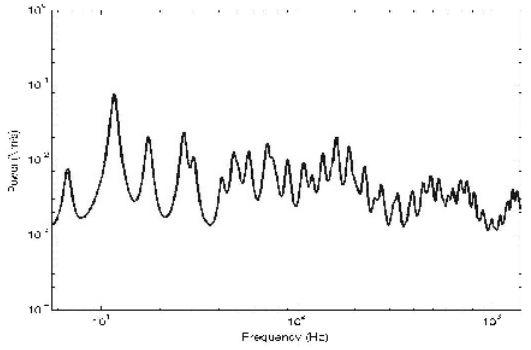

Fig. 3. Comparison of power balance for the coupled structure shown in Fig. 2 (beam excited). Power input (——) and the sum of powers dissipated in all subsystems (– – –).

Table 1. Nominal dimensions of the coupled structure shown in Fig. 2.

Beam length, L_x (m)	1.0
Beam height, h (mm)	23.7
Beam thickness, t_b (mm)	6.0
Plate width, L_y (m)	0.75
Plate thickness, t_p (mm)	6.0

Before considering experiments for the verification of the numerical model, the power balance (thus energy conservation) between subsystems is first checked. Power input for the present point excitation and the corresponding power sum dissipated in all subsystems are compared in Fig. 3. The dissipated power is calculated from the strain energy of each subsystem. One can see that the power balance holds (maximum errors of 0.0%).

The numerical results are now compared with the experiments in terms of energy and power. The experimental system is made of Acrylic Perspex. The nominal dimensions are shown in Table 1. The basic material properties such as mass per unit length, density, Young's modulus and damping loss factor are measured. A pseudo-random force was applied at beam b1 (0.36 m from the end of beam 1) using the exciter and the laser vibrometer was used to measure the velocity. A beam instead of a plate was excited to avoid the mass effect due to the force transducer, even though the mass effect is not negligible at high frequencies in such a situation. Measurement points were selected randomly over the plate (20 points) and the beams (10 points each), and used to give an estimate of the spatially averaged energy.

The energy and power refer to values normalised

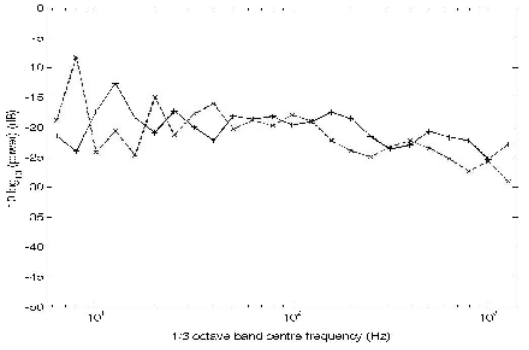

Fig. 4. Input power in one-third octave bands for the beam-plate-beam system. —|— , calculation; – × – , experiment.

by the mean square force, which is convenient when they are expressed in terms of spatial averages. The power input in one-third octave bands is shown in Fig. 4. The result of the Fourier method is in quite good agreement with that of the experiment.

A general level difference is found between the numerical model and the experiment at high frequencies. It seems to be related to the mass of the force transducer. The difference is about 4 dB at 1412 Hz.

One can find that there is a consistent frequency shift in the general trend especially above 100 Hz. It seems for example that the dip of 250 Hz in the experiment moves to 315 Hz in the numerical result. The frequency shift may be explained in terms of different boundary conditions (sliding and free) and corresponding motion of an uncoupled beam. Consider the uncoupled beam having the same beam properties. If the beam ends are sliding, then there is a natural frequency of the beam at 356.1 Hz where the beam has 4 nodal points in its bending mode ($k_b = 4\pi$). The most similar experimental motion having 4 nodal points occurs at 273 Hz in the beam where the beam ends are free (although strictly the two motions are different especially at the ends of the beam). The frequency shift occurs by about a factor of 1.30 ($= 356.1/273$) for these similar modes, which is similar to the shift seen in Fig. 4. Frequency shifts in the other peaks and dips shown in Fig. 4 may also be explained in a similar way.

The energy ratio between the various subsystems is compared. This has the advantage of reducing the effect of boundary conditions and cancelling out any mass effect. Also, the differences in response level are eliminated by comparing the energy ratios. Figure 5

shows the one-third octave band averages of the

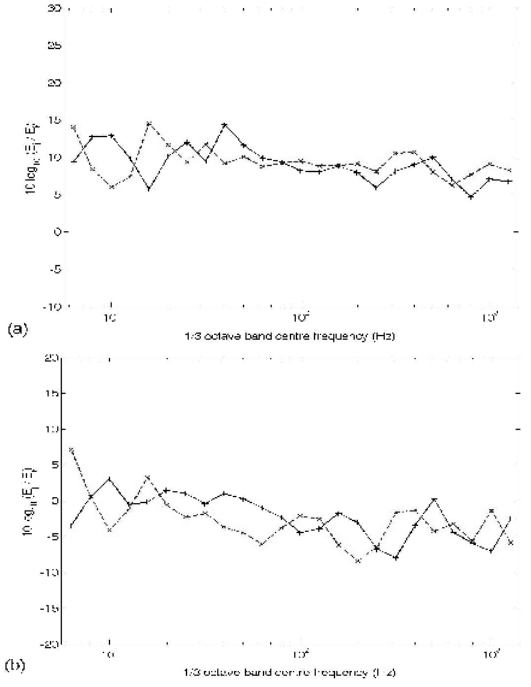

(a) energy ration E_{plate}/E_{b1} , (b) energy ratio E_{b2}/E_{b1} .

Fig. 5. Energy ratio in one-third octave bands for the two-beam-plate system. The Fourier method and experimental results for —|— , Fourier method; $-\times-$, experiment.

energy ratios between the subsystems for both the Fourier method and the experiment. It can be seen that the numerical model replicates the experimental situation well, although the frequency shift is found due to the same reason of the boundary condition as explained.

3. Energy prediction for a beam-plate-beam structure

The principal objective of SEA is to establish a model which can be used to predict the average responses of a coupled structure in terms of the gross parameters of the subsystems of the original structure. The main parameters required in this process are the subsystem dissipation loss factors and the coupling loss factors. As the system is described in terms of subsystem energies, the analysis procedure is normally carried out with a power balance equation for each of the subsystems. A structure consisting of just two subsystems is usually taken into account (Lyon and DeJong, 1995), in this case a beam-plate coupled structure. The detail backgrounds for an SEA model consisting of two subsystems are not presented here.

As it is normally assumed that the interaction between two subsystems is not affected by the presence of a third subsystem (Lyon and DeJong, 1995), using the coupling loss factors obtained from the single beam structure, it would seem possible to predict using SEA the energy of each subsystem of a beam-plate-beam coupled structure shown in Fig. 2. As the Fourier technique can also be applied to predict the response of the two-beam coupled structure this is used to give an 'exact' result for comparison. The two beams are chosen to have different dimensions initially.

3.1 SEA power balance relationships for a beam-plate-beam coupled structure

To predict the energy of a subsystem, firstly it is necessary to identify the power balance relationship in terms of a SEA model. The power balance relationships for the coupled structure consisting of three subsystems are shown in Fig. 6 and the corresponding power balance equations for the different excitation cases can be derived. In this section to avoid confusion in the notation, beam 1 is named subsystem 1, the plate is named subsystem 2 and the second beam is named subsystem 3 (or beam 3).

Note that there is no direct power transfer between subsystem 1 and subsystem 3 in the figure.

That is, as in the traditional SEA framework (Lyon and DeJong, 1995), the hypothesis is taken into account that the coupling between subsystem 1 (beam 1) and subsystem 3 (beam 3), so-called 'indirect coupling', does not exist. This is generally true because SEA assumes 'weak coupling' between two subsystems, which ensures that indirect interaction via any other subsystem is negligible (Fahy, 1994). However, it will be shown later that this may not be true for the particular coupled systems considered in the present study.

If an external force is applied to subsystem 1 as in Fig. 6 (a), using the ensemble notation '-', the power balance equations are

$$\overline{P}_{1,in}^{(1)} = \overline{P}_{1,dis}^{(1)} + \overline{P}_{12}^{(1)} \quad (27.\text{a})$$

$$\overline{P}_{12}^{(1)} = \overline{P}_{2,dis}^{(1)} + \overline{P}_{23}^{(1)} \quad (27.\text{b})$$

$$\overline{P}_{23}^{(1)} = \overline{P}_{3,dis}^{(1)} \quad (27.\text{c})$$

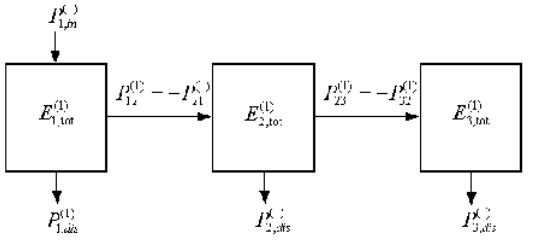

(a) Power input to subsystem 1

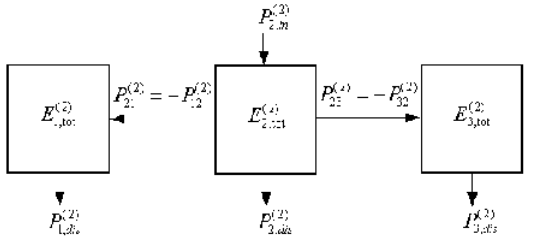

(b) Power input to subsystem 2

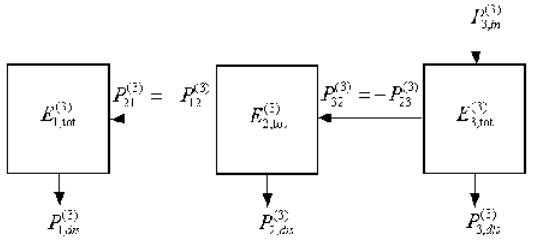

(c) Power input to subsystem 3

Fig. 6. Power balance between subsystems of the coupled structure as in Fig. 2.

where $\overline{P}_{ij}$ is the net transferred power between subsystem i and j and $\overline{P}_{in}$ and $\overline{P}_{i,dis}$ are the input power and the net dissipated power by subsystem i. The superscript indicates which subsystem is being excited.

Similarly, if the force is applied to subsystem 2 as in Fig. 6 (b), then the power balance equations are

$$\overline{P}_{2,in}^{(2)} = \overline{P}_{2,dis}^{(2)} + \overline{P}_{21}^{(2)} + \overline{P}_{23}^{(2)} \quad (28.\text{ a})$$

$$\overline{P}_{21}^{(2)} = \overline{P}_{1,dis}^{(2)} \quad (28.\text{ b})$$

$$\overline{P}_{23}^{(2)} = \overline{P}_{3,dis}^{(2)} . \quad (28.\text{ c})$$

Also, if the force is applied to subsystem 3 as in Fig. 6 (c), then the power balance equations are

$$\overline{P}_{3,in}^{(3)} = \overline{P}_{3,dis}^{(3)} + \overline{P}_{32}^{(3)} \quad (29.\text{ a})$$

$$\overline{P}_{32}^{(3)} = \overline{P}_{2,dis}^{(3)} + \overline{P}_{21}^{(3)} \quad (29.\text{ b})$$

$$\overline{P}_{21}^{(3)} = \overline{P}_{1,dis}^{(3)} . \quad (29.\text{ c})$$

Introducing the relationship between the dissipated power and stored energies i.e. $\overline{P}_{i,dis} = \eta_i \omega \overline{E}_i$, with η_i the internal loss factors, and $\overline{P}_{ij} = \eta_{ij}\omega\overline{E}_i - \eta_{ji}\omega\overline{E}_j$, with η_{ij} the coupling loss factors, then the power balance equations corresponding to Eqs.(27)~(29) can be expressed as follows.

$$\overline{P}_{1,in}^{(1)} = \omega\left[\left(\eta_1^{(1)} + \eta_{12}^{(1)}\right)\overline{E}_1^{(1)} - \eta_{21}^{(1)}\overline{E}_2^{(1)}\right]. \quad (30.\text{ a})$$

$$0 = \omega\left[-\eta_{12}^{(1)}\overline{E}_1^{(1)} + \left(\eta_2^{(1)} + \eta_{21}^{(1)} + \eta_{23}^{(1)}\right)\overline{E}_2^{(1)} - \eta_{32}^{(1)}\overline{E}_3^{(1)}\right]. \quad (30.\text{ b})$$

$$0 = \omega\left[\left(\eta_3^{(1)} + \eta_{32}^{(1)}\right)\overline{E}_3^{(1)} - \eta_{23}^{(1)}\overline{E}_2^{(1)}\right]. \quad (30.\text{ c})$$

$$\overline{P}_{2,in}^{(2)} = \omega\left[-\eta_{12}^{(2)}\overline{E}_1^{(2)} + \left(\eta_2^{(2)} + \eta_{21}^{(2)} + \eta_{23}^{(2)}\right)\overline{E}_2^{(2)} - \eta_{32}^{(2)}\overline{E}_3^{(2)}\right]. \quad (31.\text{ a})$$

$$0 = \omega\left[\left(\eta_1^{(2)} + \eta_{12}^{(2)}\right)\overline{E}_1^{(2)} - \eta_{21}^{(2)}\overline{E}_2^{(2)}\right]. \quad (31.\text{ b})$$

$$0 = \omega\left[\left(\eta_3^{(2)} + \eta_{32}^{(2)}\right)\overline{E}_3^{(2)} - \eta_{23}^{(2)}\overline{E}_2^{(2)}\right]. \quad (31.\text{ c})$$

$$\overline{P}_{1,in}^{(1)} = \omega\left[\left(\eta_3^{(3)} + \eta_{32}^{(3)}\right)\overline{E}_3^{(3)} - \eta_{23}^{(3)}\overline{E}_2^{(3)}\right]. \quad (32.\text{ a})$$

$$0 = \omega\left[-\eta_{12}^{(3)}\overline{E}_1^{(3)} + \left(\eta_2^{(3)} + \eta_{21}^{(3)} + \eta_{23}^{(3)}\right)\overline{E}_2^{(3)} - \eta_{32}^{(3)}\overline{E}_3^{(3)}\right]. \quad (32.\text{ b})$$

$$0 = \omega\left[\left(\eta_1^{(3)} + \eta_{12}^{(3)}\right)\overline{E}_1^{(3)} - \eta_{21}^{(3)}\overline{E}_2^{(3)}\right]. \quad (32.\text{ c})$$

In Eqs. (30)~(32), powers and energies are time-averaged quantities, η_1, η_2 and η_3 are the damping loss factors of the corresponding subsystems.

3.2 Effective CLF

Although the power balance equations are evaluated strictly in terms of ensemble averages, in real applications it is often difficult to realise an ensemble. Alternatively the power balance equations hold for an individual realisation and a CLF-like term may be obtained for a particular realisation. This is referred to as the effective CLF $\hat{\eta}_{ij}$ (Park et al., 2004). Thus, the effective coupling loss factors (CLFs) are obtained instead of the exact CLFs based on an average over an ensemble of realisations. Assuming $\hat{\eta}_{ij}^{(i)} = \hat{\eta}_{ij}^{(j)}$, the effective CLFs can be obtained from Eqs. (30)~

(32). Introducing a matrix form results in Eq. (33).

$$\omega^{-1}\mathbf{P} = [\eta]\mathbf{E} \tag{33}$$

where

$$\mathbf{P} = \begin{bmatrix} P_{1,in}^{(1)} & 0 & 0 \\ 0 & P_{2,in}^{(2)} & 0 \\ 0 & 0 & P_{3,in}^{(3)} \end{bmatrix} \tag{34}$$

$$\mathbf{E} = \begin{bmatrix} E_1^{(1)} & E_1^{(2)} & E_1^{(3)} \\ E_2^{(1)} & E_2^{(2)} & E_2^{(3)} \\ E_3^{(1)} & E_3^{(2)} & E_3^{(3)} \end{bmatrix} \tag{35}$$

$$[\eta] = \begin{bmatrix} \eta_1 + \hat{\eta}_{12} & -\hat{\eta}_{12} & 0 \\ -\hat{\eta}_{21} & \eta_2 + \hat{\eta}_{21} + \hat{\eta}_{23} & -\hat{\eta}_{23} \\ 0 & -\hat{\eta}_{32} & \eta_3 + \hat{\eta}_{32} \end{bmatrix}. \tag{36}$$

Note that, here, the power flows and the stored energies are presented by space-averaged and frequency-averaged representation such as the octave band frequency average and therefore the frequency ω is the centre frequency of the corresponding octave band.

3.3 Prediction of subsystem energy

In Eq. (36), one can see that the matrix contains only the effective CLFs between subsystems 1 and 2 or subsystems 2 and 3. These CLFs will be obtained from a beam-plate system. Therefore the energies E can be predicted using the CLFs earlier.

$$\mathbf{E} = \omega^{-1}[\eta]^{-1}\mathbf{P}. \tag{37}$$

In fact, in order to obtain the energy terms it is necessary to know the input powers of the beam-plate-beam coupled structure. However, by scaling the total input power to unity, the energy normalised by the input power can be found from the coupling loss factors of the beam-plate coupled structure where excitation is applied separately to one of the subsystems and solving Eq.(33) for the known power input and coupling matrix.

3.4 Numerical analysis of a beam-plate structure

The effective CLFs are firstly obtained for the single beam coupled structure shown in Fig. 7, so that they can be used to predict the subsystem energies of a beam-plate-beam coupled structure. The material properties and the dimensions used are presented in Table 2.

Table 2. Material properties and dimensions of the baseline model shown in Fig. 7.

Material	Perspex	Height of beam, h (mm)	68.0
Young's modulus, E (GNm^{-2})	4.4	Beam length, L_x (m)	3.0
Poisson's ratio, ν	0.38	Plate width, L_y (m)	0.75
Density, ρ (kgm^{-3})	1152.0	Thickness, t (mm)	5.9
DLF of the beam, η_1	0.03	DLF of the plate, η_2	0.01

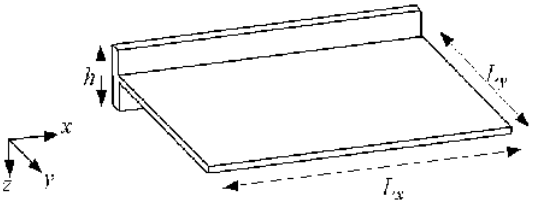

Fig. 7. A built-up structure consisting of a finite beam attached to a finite rectangular plate.

The Fourier technique is used to evaluate dynamic responses. The ends of the beam are assumed to be sliding and the plate is also assumed to be sliding along the edges $x = 0$, $x = L_x$ and along the coupling junction $y = 0$, while the opposite edge to the junction, $y = L_y$ is assumed to be pinned. Note that, in order to obtain the effective CLFs $\hat{\eta}_{12}$ (beam to plate) and $\hat{\eta}_{21}$ (plate to beam), it is necessary to consider both the beam-excited and the plate-excited cases simultaneously, and also assuming $\hat{\eta}_{ij}^{(1)} = \hat{\eta}_{ij}^{(2)}$.

SEA was originally formulated for random forcing, so-called 'rain-on-the-roof' forcing, and the response of the system to the rain-on-the-roof forcing is taken to be the equivalent to the average response to the point forcing over all possible excitation locations (Lyon and DeJong, 1995). In the present study, 20 excitation points are chosen randomly on both the beam and the plate and each is used to obtain total energy of the subsystem and total power input. The energy corresponding to each subsystem is obtained from the maximum strain energy.

Frequency bands such as 1/3 octave or octave bands can be chosen for estimating the CLF, and in the present study the octave band is used. This is because it is necessary to include a sufficient number

of modes, especially for the beam which is much stiffer than the plate. Also, for obtaining enough information concerning coupling, an overlapping band technique is used, so that the data can be presented with a resolution of 1/3 octave bands.

The calculated effective CLFs $\hat{\eta}_{12}$ and $\hat{\eta}_{21}$ are shown in Fig. 8. It can be seen that negative values of CLFs are found for frequency bands of 16, 20 and 25 Hz. This is because there are not enough modes in the beam and correspondingly not enough energy in the beam. In fact, there is no mode between 11 and 35 Hz for the present coupled beam and the coupled structure is dominated by the plate motion. For example, at 21 Hz, the dominant mode of the coupled structure is flexural mode of the plate where the wavelength is about $\lambda \approx 1.0$ m. Meanwhile the beam remains in rigid motion. Therefore, the small modal energy of the beam results in the negative value of the CLF. It is generally recommended to have at least 5 modes in a band (Fahy and Mohammed, 1992).

One of the general hypotheses of SEA is that 'weak coupling' is present. If the Smith criterion is used, where the coupling is considered weak when the CLF η_{12} is smaller than the DLF of the source subsystem η_1, that is $\eta_{12} < \eta_1$ (Smith Jr, 1979), then the baseline model seems clearly to be in a strong coupling regime for the beam excited case, as seen in Fig. 8. Note that the DLF of the beam (source structure) η_1 is 0.03 and the effective CLF $\hat{\eta}_{12}$ is about 0.1. Meanwhile, the plate excited case seems to be weakly coupled at high frequencies.

3.5 Numerical analysis of a beam-plate-beam structure

In this section, using the effective CLFs obtained based on the beam-plate structure, the energies normalised by the total input powers of the beam-plate-beam structure as in Fig. 2 are predicted and examined. The dimensions of the beams in the corresponding beam-plate-beam coupled structure are shown in Table 3 and the other dimensions are the same as shown in Table 2 for the beam-plate structure. The height of beam 3 is arbitrarily chosen so that it has different wavenumbers from beam 1 ($h_1 = 68$ mm and $h_3 = 50$ mm), and it is expected that their modal behaviours are different. The uncoupled wavenumber of the 50 mm height beam is 17 % greater than that of the 68 mm height beam.

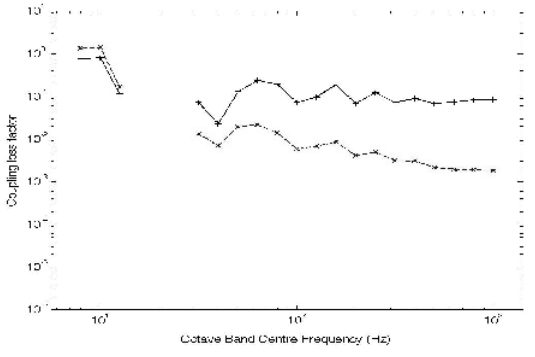

Fig. 8. Effective CLFs of the Baseline model. —|—, $\hat{\eta}_{12}$; —×—, $\hat{\eta}_{21}$.

The numerical calculation for the effective CLFs of a coupled structure where the beam height is 68 mm is carried out using the Fourier transform approach and then a 50 mm height beam case is considered. Then these effective CLFs are used to predict the normalised energy using Eq. (37) where excitation is applied to one of the subsystems. It is necessary to mention that the boundary conditions for the opposite edge of the plate coupled to a single beam is assumed to be a pinned condition as before, while the edges of a plate coupled to two beams are sliding. Although their boundary conditions are not the same, it is assumed that the effect of the boundary condition is small, especially at high frequencies.

For comparison with the SEA predicted normalised energies, the comparable normalised energies are obtained directly from the beam-plate-beam structure using the Fourier technique. The responses are averaged over 20 point excitations separately applied to one of the subsystems only. The analytical solution for the motion of such a beam-plate-beam structure where a beam is excited can be found similarly as in Chapter 2.

Firstly, the normalised energies when subsystem 1 (beam 1) is excited are shown in Fig. 9. The same symbols in the lines are used to distinguish each subsystem. The thick lines indicate results obtained directly from the Fourier approach while the thin lines are obtained from the SEA model.

Table 3. Dimensions of the built-up structure shown in Fig. 2.

	Beam 1 (subsystem 1)	Beam 3 (subsystem 3)
Height of the beam, h (mm)	68.0	50.0
Thickness, t (mm)	5.9	5.9
Loss factor of the beam, η_1	0.03	0.03

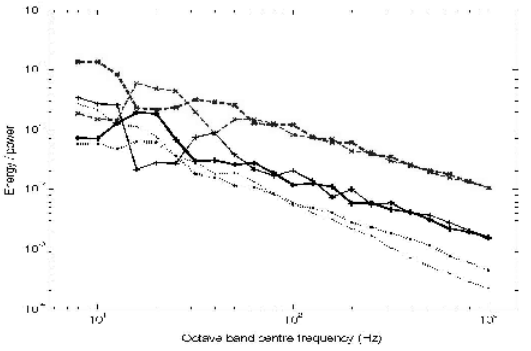

Fig. 9. Energies normalised by total input power (h_1=68 mm, h_3=50 mm. Beam 1 excited). Thick lines directly from the beam-plate-beam structure and thin lines based on the effective CLFs and solving the SEA model. —+— , beam 1; – × – , plate; ··· • ··· , beam 3.

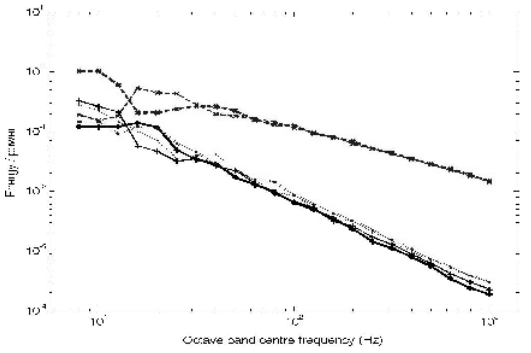

Fig. 10. Energies normalised by total input power (h_1=68 mm, h_3=50 mm. Plate excited). Thick lines directly from the beam-plate-beam structure and thin lines based on the effective CLFs and solving the SEA model. —+— , beam 1; – × – , plate; ··· • ··· , beam 3.

Significant differences are found at low frequencies. One can recall that the effective CLFs of the single beam structure show negative values around 20 Hz (see section 3.4). The lowest frequency bound where an effective CLF can be predicted is about 30 Hz in the present beam-plate coupled system considered. Thus, it can be said that the corresponding effective CLFs are not appropriate for the prediction of energy. However, the energies of each subsystem are in good agreement at higher frequency, especially for beam 1 and the plate. There is some difference for the energy of beam 3. Note that this is the case when beam 1 is excited and this has higher response at high frequencies than the other beam.

For the plate-excited case, the corresponding results are shown in Fig. 10. It can be seen that they are generally in good agreement for all subsystems. The plate has the greatest response and the two beams, although slightly dissimilar, are significantly lower in response and not differing very much. This is probably the case of best agreement using the SEA model and the exact beam-plate-beam analysis.

The case for excitation on beam 3 is shown in Fig. 11. The normalised energies are generally in good agreement for beam 3 and the plate. However there is a big difference between the SEA prediction and the exact result for the non-excited beam (beam 1).

From Figs. 9 - 11, one can see that the differences between the SEA and exact predictions for the normalised energies are greatest when the response of the non-excited beam subsystem is calculated for excitation on the other beam. Otherwise, for the case when the plate is excited, they show very good agreement. This may be due to the indirect coupling

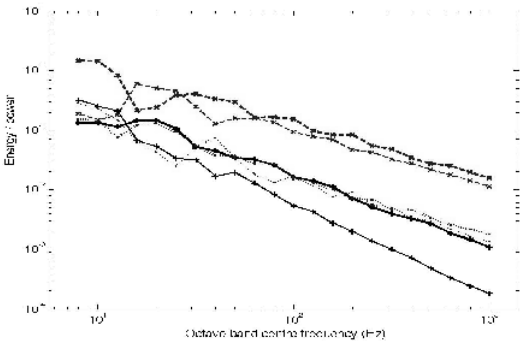

Fig. 11. Energies normalised by total input power (h_1=68 mm, h_3=50 mm. Beam 3 excited). Thick lines directly from the beam-plate-beam structure and thin lines based on the effective CLFs and solving the SEA model. —+— , beam 1; – × – , plate; ··· • ··· , beam 3.

between beam 1 and beam 3.

Previously it was mentioned that traditional SEA does not consider indirect coupling for a weakly coupled system. Whilst, one can recall that the beam-plate coupled system discussed in the previous section where the beam is excited may be regarded as a strongly coupled system. Consequently, the hypothesis that there is no indirect coupling in the present beam-plate-beam structure is not likely true. That is, although they are not coupled physically, in fact it seems true that there is a coupling so that power flow occurs between two indirectly coupled beams in an 'SEA sense'. One may also recall that the power balance hold for the Fourier model of the beam-plate-beam system (see section 2.2). Thus, it should be noticed that whenever the indirect coupling is mentioned it is always in an 'SEA sense'.

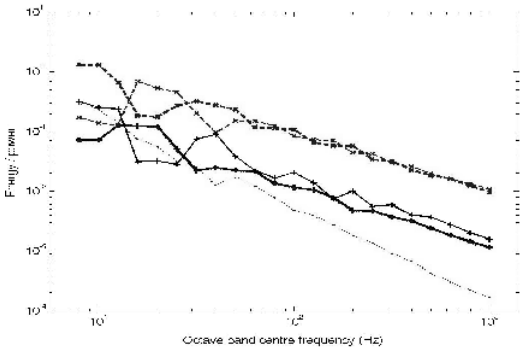

Fig. 12. Energies normalised by total input power (h_1=68 mm, h_3=67 mm. Beam 1 excited). Thick lines directly from the beam-plate-beam structure and thin lines based on the effective CLFs and solving the SEA model. —+—, beam 1; – × –, plate; ⋯•⋯, beam 3.

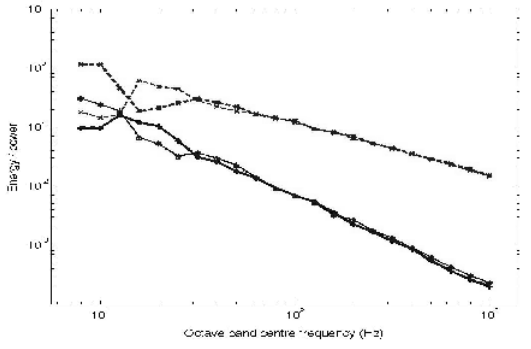

Fig. 13. Energies normalised by total input power (h_1=68 mm, h_3=67 mm. Plate excited). Thick lines directly from the beam-plate-beam structure and thin lines based on the effective CLFs and solving the SEA model. —+—, beam 1; – × –, plate; ⋯•⋯, beam 3.

Such an effect was explained by Heron (1997), who introduced Advanced Statistical Energy Analysis (ASEA). ASEA allows for coupling between subsystems that are physically separate by a so-called 'tunnelling mechanism' in which, even though the subsystems are physically separated from each other coupling may exist in an SEA sense. An additional explanation follows later in this section.

Further investigation of this effect is carried out for the case when both beams have similar modal energies. To realise this situation, the height of beam 3 is modified to 67 mm, which is close to that of beam 1 but not identical. Firstly, the results for excitation on beam 1 are shown in Fig. 12. It can be seen that the difference in the normalised energy of beam 3 is greater than that shown in Fig. 9. Moreover, the response of beam 1 is slightly lower than that

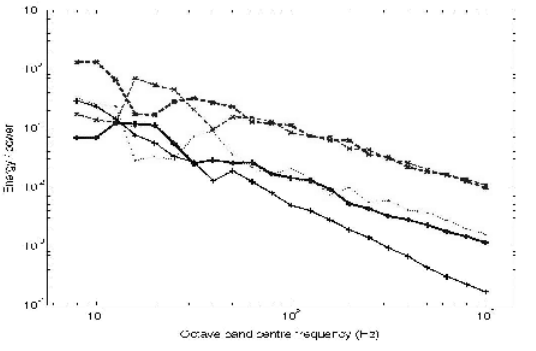

Fig. 14. Energies normalised by total input power (h_1=68 mm, h_3=67 mm. Beam 3 excited). Thick lines directly from the beam-plate-beam structure and thin lines based on the effective CLFs and solving the SEA model. —+—, beam 1; – × –, plate; ⋯•⋯, beam 3.

predicted by the SEA model.

However, if the plate is excited, good agreement is found between the results predicted using the CLFs and SEA and those directly obtained from the beam-plate-beam Fourier analysis as shown in Fig. 13.

Finally, the results for excitation on beam 3 are shown in Fig. 14. One can see that the difference for the response of beam 1 again increases as frequency increases.

Therefore, from Figs. 12-14, it can be inferred that the indirect coupling effect plays an important role for such a beam-plate-beam coupled structure. To get accurate results using the SEA model it is insufficient to use only the direct effective CLFs calculated between a plate and a beam.

The emphasis should be placed on that the indirect coupling mentioned here does not mean that energy flows from the excited beam to the other beam without passing through the plate connecting two subsystems (Fahy, 1994). It does mean that the SEA framework does not include all mechanism of energy flow that exists in the present beam-plate-beam system. A study that considers indirect coupling could be carried out, for example, using the ASEA mentioned. This will be the subject of a future study.

4. Conclusions

Coupled systems of beams and a plate have been investigated in the SEA framework.

The power and energy of the subsystems are obtained from the Fourier technique. The numerical results of this method have been experimentally verified.

Then, using the Fourier model, the effective coupling loss factor (CLF) of a beam-plate coupled structure has been investigated in terms of the SEA framework. Although the actual CLF is defined in terms of an ensemble average, the frequency average technique is used here instead of the ensemble average. The CLFs are presented in overlapping octave frequency bands. It seems that the beam-plate model behaves as a strongly coupled system for power flow from the beam to the plate.

An attempt has been made to predict the subsystem energy of the beam-plate-beam structure using the effective CLFs previously obtained from the beam-plate structure. The energy normalised by input power has been compared with that directly obtained from the Fourier approach. They are generally in good agreement at high frequencies for the plate-excited situation. However, when one beam is excited, the normalised energy of the other beam shows some discrepancy. It seems that this may occur due to the indirect coupling effect in an SEA sense between the two beams. The discrepancy is largest when the beams are similar. A further study remains for this.

Nomenclature

B, C	:	Wave amplitude in a plate (m)
D	:	Beam stiffness (Nm^2); plate stiffness (Nm)
E	:	Young's modulus of elasticity (N/m^2); energy
F_i	:	Spatial Fourier transform of force f_i (N/m)
L_x	:	Length of a beam (m)
L_y	:	Width of a plate (m)
P	:	Power
W	:	Spatial Fourier transform of displacement w (m)
f	:	Frequency (Hz)
f_i	:	Force per unit length (N/m)
h	:	Height of a beam
i	:	$\sqrt{-1}$
k	:	Wavenumber
k_p	:	Uncoupled free wavenumber in a plate
k_x	:	Coupled travelling trace wavenumber of a beam
k_y	:	Trace wavenumber in a plate
m_b'	:	Mass per unit length of a beam (kg/m)
m_p''	:	Mass per unit area of a plate (kg/m^2)
t	:	Thickness (m)
w	:	Displacement (m)
x, y, z	:	Co-ordinates
α	:	Constant
β	:	Constant
δ	:	Dirac delta function
η	:	Dissipation loss factor (-)
η_{ij}	:	Ensemble average coupling loss factor
$\hat{\eta}_{ij}$	:	Effective coupling loss factor
λ	:	Wavelength (m)
ν	:	Poisson's ratio
ω	:	Radian frequency (rad/s)

References

Bies, D. A. and Hamid, S., 1980, "*In Situ* Determination of Loss and Coupling Loss Factors by the Power Injection Method," *Journal of Sound and Vibration*, Vol. 70, pp. 187~204.

Craik, R. J. M., 1996, *Sound Transmission through Buildings using Statistical Energy Analysis*, Gower Publishing, Aldershot.

ESDU 99009, "An Introduction to Statistical Energy Analysis".

Fahy, F. J. and Mohammed, A. D., 1992, "A Study of Uncertainty in Applications of SEA to Coupled Beam and Plate Systems, Part 1: Computational Experiment," *Journal of Sound and Vibration*, Vol. 158, pp. 45~67.

Fahy, F. J., 1994, "Statistical Energy Analysis: a Critical Overview," *Philosophical Transactions of the Royal Society of London, series A*, Vol. 346, pp. 431~447.

Grice, R. M. and Pinnington, R. J., 1999, "A Method for the Vibrational Analysis of Built-up Structures, Part 1: Introduction and analytical analysis of the plate-stiffened beam," *Journal of Sound and Vibration*, Vol. 230, pp. 825~849.

Heron, K. H., 1997, "Advanced Statistical Energy Analysis," *Philosophical Transactions of the Royal Society of London, series A*, Vol. 346, pp. 501~510.

Jayachandran, V. and Bonilha, M. W., 2003, "A Hybrid SEA/Modal Technique for Modelling Structural-acoustic Interior Noise in Rotorcraft," *Journal of Acoustical Society of America*, Vol. 113, pp. 1448~1454.

Ji, L., Mace, B. R. and Pinnington, R. J., 2003, "Estimation of Power Transmission to a Flexible Receiver from a Stiff Source Using a Power Mode Approach," *Journal of Sound and Vibration*, Vol. 268, pp. 525~542.

Kompella, M. S. and Bernhard, B. J., 1993, "Measurement of the statistical variation of structural-acoustic characteristics of automotive vehicles," In Proc. SAE noise and vibration Conf., Society of Automotive Engineers, Warrendale.

Lyon, R. H. and DeJong, R. G., 1995, *Theory and Application of Statistical Energy Analysis*, Butterworth-Heinemann, Boston.

Mace, B. R., 1994, "On the Statistical Analysis Hypothesis of Coupling Power Proportionality and Some implications of its failure," *Journal of Sound and Vibration*, Vol. 178, pp. 95~112.

Noguchi, Y., Doi, T., Tada, H. and Misaji, K., 2006, "Development of a lightweight Sound Package for 2006 brand-new vehicle categorized as C," *SAE Paper 2006-01-0710*.

Park, W. S., Thompson, D. J. and Ferguson, N. S., 2004, "The influence of modal behaviour on the energy transmission between two coupled plates," *Journal of Sound and Vibration*, Vol. **276**, pp. 1019~1041.

Smith Jr, P. W., 1979, "Statistical Models of Coupled Dynamical Systems and the Transition from Weak to Strong Coupling," *Journal of Acoustical Society of America*, Vol. 65, pp. 695~698.

Strasberg, M. and Feit, D., 1996, "Vibration Damping of Large Structures Induced by Attached Small Resonant Structures," *Journal of the Acoustical Society of America*, Vol. 99, pp. 335~344.

Wester, E. C. N. and Mace, B. R., 1996, "Statistical Energy Analysis of Two Edge-coupled Rectangular Plate: Ensemble Averages," *Journal of Sound and Vibration*, Vol. 193, pp. 793~822.